JTTEE5 22:588–598
DOI: 10.1007/s11666-013-9929-4
1059-9630/$19.00 © ASM International

Thermal Plasma Spraying Applied on Solid Oxide Fuel Cells

D. Soysal, J. Arnold, P. Szabo, R. Henne, and S.A. Ansar

(Submitted September 29, 2012; in revised form March 28, 2013)

Solid oxide fuel cells (SOFCs), attractive for diverse applications in a broad range from small portable and auxiliary power units, up to central power systems, are conventionally produced by sintering methods. However, plasma spraying promises some advantages particularly for cells with metal support. In the present paper, research activities conducted in recent years at DLR as well as latest developments on plasma sprayed functional layers for SOFC as cathodes, electrolytes, and anodes are reported. Power densities of more than 800 mW/cm^2 were achieved for plasma sprayed single cells of 12.56 cm^2 size, and 300 mW/cm^2, respectively, with a 250 W stack made of 10 cells. These values were attained at 0.7 V and 800 °C, with H_2:N_2 = 1:1 as fuel gas and air as oxidizing gas. Furthermore, continuous operation of more than 5000 h was attained with a plasma sprayed metal-supported SOFC stack which could also withstand more than 30 redox and thermal cycles.

Keywords degradation, long-term stability, metal-supported SOFC, plasma sprayed functional layers, suspension plasma spraying

1. Fuel Cells—Devices Not Limited to Only One Single Application

Present times are characterized by a general change in the energy supply. The scarcity of fossil resources requires a considerably higher efficiency in their use. At the same time a rapid increase of using renewable energy sources like solar radiation and wind can be observed. Therefore, hydrogen will become of increasing significance in the future as a carrier of energy for a society oriented to regenerative energy supply. It is storable and transportable, can be manufactured in a simple way by means of electrolysis and can be used to produce thermal and electrical power in a highly efficient and environmentally friendly form by fuel cells. As fuel cells transform combustion gas consisting mainly of hydrogen not only into thermal and electrical energy, but also in water and well-defined harmless exhaust emission, they can be used multi-functionally. This is shown in Fig. 1 using the example of applications in aviation. In addition to an auxiliary power unit (APU) for on-board electricity and replacing the ram air turbine (RAT) for the emergency power supply, the fuel cell may serve to reduce considerably the extra load of water before the start since service water needed in lavatory, e.g., is produced by the fuel cell during the flight. Moreover, the exhaust gases of the fuel cell can be filled into the tanks of the airplane (being located in the wings) and, therefore, the development of explosive gas mixtures can be suppressed as the tank is getting depleted (''inertisation'').

There are a number of different types of fuel cells operating from ambient temperature up to about 1000 °C with differences in materials, structure, function, geometry, properties and required combustion gases. Solid oxide fuel cells (SOFCs) with operating temperatures above 600 °C can be run with a variety of fuels without any elaborate reforming needed. This makes them attractive for very different applications in a broad range from small portable and APUs, combined heat and power suppliers in houses up to central power systems. A special type of cells is the so-called metal-supported solid oxide fuel cell (MS-SOFC, Fig. 2a). Primarily MS-SOFCs have been developed for use in the automotive sector. Therefore, development goals are lowest possible weight with highest possible energy density and quick and uniform start-up. In contrast with anode- or electrolyte-supported fuel cells a porous metal substrate performs the mechanical load-bearing function of the cell (Fig. 2b).

Conventionally SOFCs are produced by sintering methods which means in general long processing times between 10 and 20 h with sintering temperatures notably above 1000 °C to get the desired mechanical quality. In case of MS-SOFC, high temperature sintering may cause degradation of metallic components and limits the choice of suitable materials and geometries. In contrast, adapted plasma spray techniques (Ref 1-3) offer some distinct advantages for metal-supported cells in terms of limiting substrate temperatures. Thermal degradation and temperature dependent interdiffusion between materials can be suppressed. Besides production of active layers (electrodes or electrolytes) plasma sprayed coatings can also be applied for corrosion protection (Ref 4), for insulating between cell components, and for sealing in SOFC stacks (Ref 5). Plasma spraying offers high production rates that

D. Soysal, J. Arnold, P. Szabo, R. Henne, and **S.A. Ansar**, German Aerospace Center (DLR), Stuttgart, Germany. Contact e-mail: johannes.arnold@dlr.de.

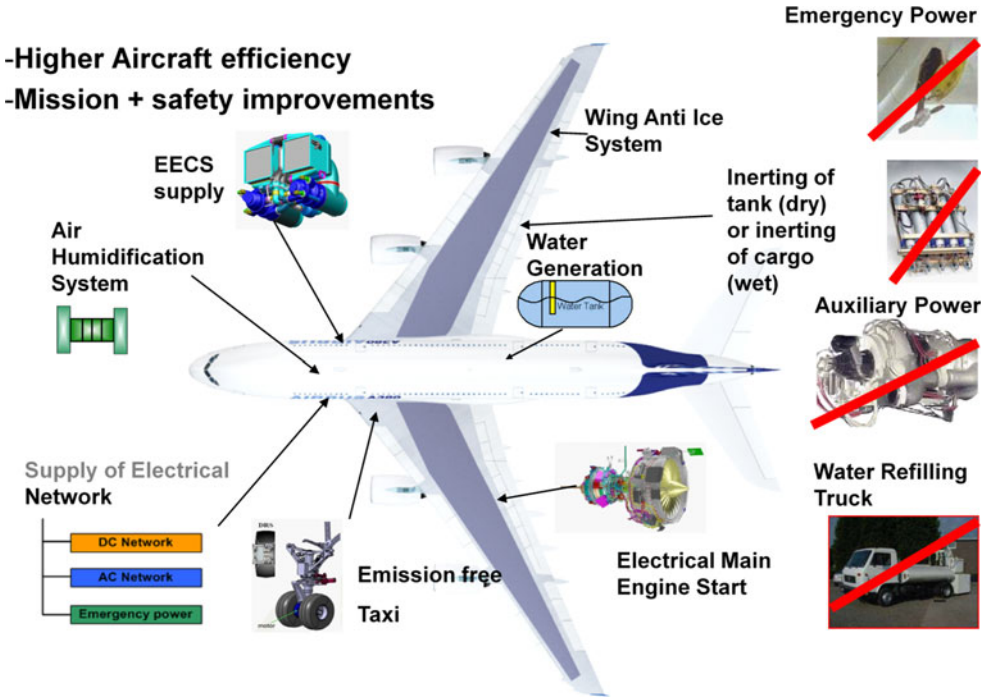

Fig. 1 Multifunctional applications of the fuel cell in aviation (EECS = Electrical Environmental Control System)

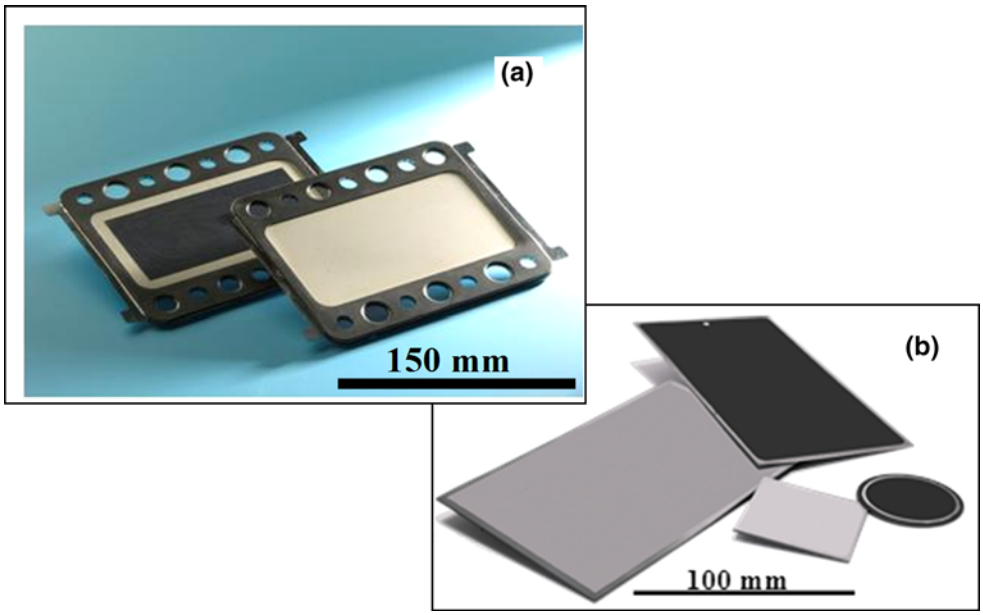

Fig. 2 Photographs of (a) two SOFCs, (b) different metal substrates (uncoated and plasma sprayed)

have the potential to lower production costs and good scalability favoring commercialization of SOFCs (Ref 6). This paper presents the research activities and the latest results achieved at DLR in recent years on development of plasma sprayed functional layers for MS-SOFCs. Main objectives of the work were to improve performance and durability of the cells by systematic enhancement in the processing conditions, incorporating sub-micrometer- and nanometer-sized functional layers.

2. Structure and Operation of SOFCs and Plasma Spraying Applied to It

The electrochemically active part of a high temperature SOFC consists in principle of three layers (Fig. 3a):

- an air electrode, where oxygen is reduced to double negatively charged oxygen ions by up-taking of electrons,

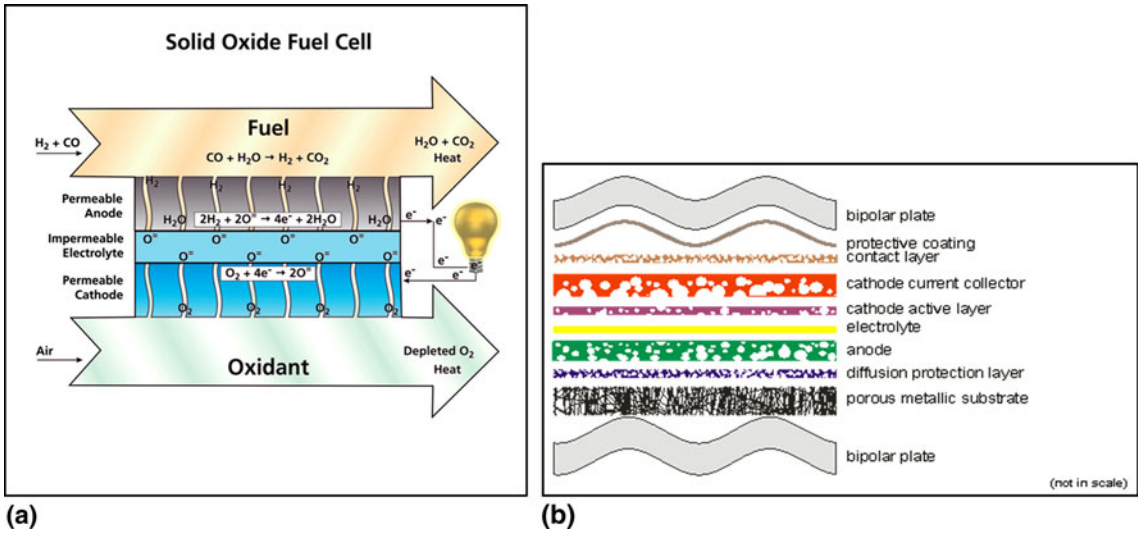

Fig. 3 (a) Operating mode of an SOFC, (b) scheme of functional layers of an MS-SOFC

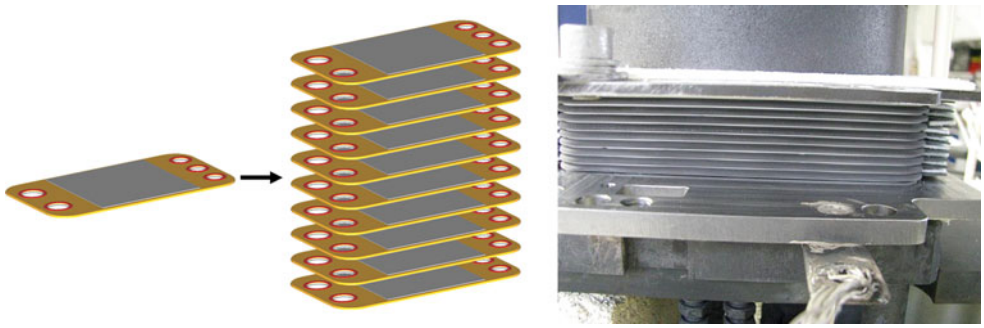

Fig. 4 MS-SOFC stack built of 10 single cells

- an electrolyte, conducting oxygen ions at higher temperatures, and
- an anode, where the fuel is oxidized and electrons are set free which return via an external load to the cathode, generating useful electrical power.

Due to the high operating temperatures of about 800 °C further components are necessary. For instance, diffusion limiting layers between different cell parts and oxidation preventing layers for the metallic interconnects (Fig. 3b). Cells typically are operated at 200 to 300 mA/cm^2 loads and the desired electrical power of a fuel cell generator is achieved by means of a series connection of identical cells (so-called ''stacking'', Fig. 4). For stack designs with reactive solder as sealing, electrically insulating layers are needed (Ref 7). Although plasma spraying is applicable and is used for production of all layers described above, in the following only development activities for the electrochemically active part of the SOFC (''the three layers'') will be specified.

Materials for the core of such cells are mostly of ceramic type: typically perovskites for the cathodes, yttria stabilized zirconia (YSZ) for the electrolyte and a mixture (cermet) of Ni and YSZ for the anode. Anode and cathode have to show suitable porosity with extended length of so-called triple phase boundaries (TPB) ensuring good access for gases and their reaction at the surfaces, whereas the electrolyte has to be dense and gas-tight, and as thin as possible to possess low resistivity for conducting the oxygen ions.

3. Plasma Spraying of Functional Layers for SOFC

SOFCs can be manufactured by atmospheric plasma spraying (APS) (Ref 8). However, for denser ceramic coatings better melting and higher particle velocities are favorable. For this reason, special plasma spraying equipment has been developed and used at DLR. Fast plasma jet and spray material velocities which are needed for dense electrolyte layers were realized by using a direct current (DC) torch with Laval like contoured anodes. The torch was integrated into a low pressure chamber (Ref 6, 9). To fabricate SOFC electrode layers a three-cathode plasma gun TriplexPro 200 (Sulzer Metco,

Fig. 5 Liquid feeding system developed at DLR with touch-screen controls and online diagnostic support

Switzerland) was applied under APS conditions. Besides standard-sized powder particles (20-60 μm) suspensions with sub-micrometer particles were alternatively injected. An in-house developed liquid injection system (Fig. 5) for suspension plasma spraying (SPS) as well as for solution precursor plasma spraying (SPPS) was adapted to get denser electrolyte coatings as well as electrode coatings with higher TPBs.

On-line diagnostic tools, employed to correlate processing parameters with the plasma jet characteristics and in-flight particles parameters, included:

- an enthalpy probe from Tekna Plasma System Inc. (Canada) for measurement of plasma enthalpy, temperature, and composition,
- Accuraspray from Tecnar (Canada) for measurement of (median) velocity and temperature of the particle jet in the plasma.

Properties of the functional layers were evaluated by employing electrochemical testing coupled with impedance spectroscopy (Ref 10), gas permeability and leak rate measurements as well as a four point dc resistivity method (Ref 11).

Additional analytic methods that have been used to characterize SOFC layers are scanning electron microscopy of powders as well as of fractured and polished samples of deposits, X-ray diffraction (XRD) measurements conducted by diffractometry in a BRAGG-BRENTANO test assembly, and coefficient of thermal

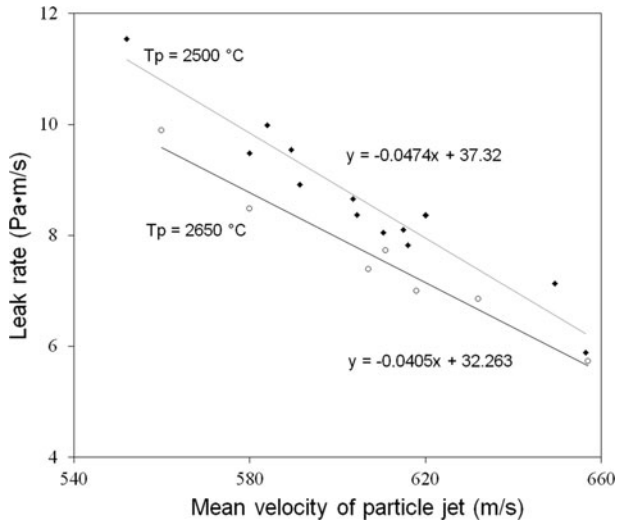

Fig. 6 Leak rate values of 8YSZ deposits as function of mean velocity and temperature of particle jet measured by Accuraspray at 300 mm standoff distance of the particle plume axis

expansion (CTE) measurements from room temperature up to 1050 °C under constant flow of air performed with a dilatometer.

3.1 Vacuum Plasma Sprayed Electrolyte Layers

Much of the research carried out on electrolytes of SOFCs is oriented to improve its ionic conductivity and, concurrently, to lower operating temperatures. Although there has been an extensive study of alternative solid electrolyte materials (like scandium doped zirconia (ScSZ), gadolinia-doped ceria (CGO), lanthanum gallate-based perovskites (e.g., LSGM), or others (Ref 12)), the most commonly used electrolyte material in SOFCs is still zirconia stabilized with 8 mol% of yttria (8YSZ) due to its better stability and lower electronic conductivity at elevated temperatures compared to other electrolyte materials (Ref 13). However, to reduce the resistivity to oxygen ion diffusion in 8YSZ, either higher operating temperature or thinner electrolyte layers are options. For operating temperatures of 800 °C and below, production of thin electrolyte layers that remain hermetic is the main challenge for the plasma spray process.

Using a D-optimal design of experiment (DOE), influence of different 8YSZ feedstock powders and plasma spray parameters were examined on deposition efficiency, gas-tightness and electrochemical behavior of vacuum plasma sprayed (VPS) electrolytes (Ref 14). In-flight particle surface temperature and average velocity, measured by on-line particle diagnostics, were correlated with plasma and deposit properties. It was concluded that the influence of particle velocity is four times higher on open porosity of the deposit than the particle temperature (Fig. 6). Owing to this development thickness and area-related leak rate values of plasma sprayed 8YSZ deposits could be reduced from 65 to 35 μm and from 15.2 to 1.7 Pa m/s, respectively, which consequently resulted in lower ohmic resistance and higher

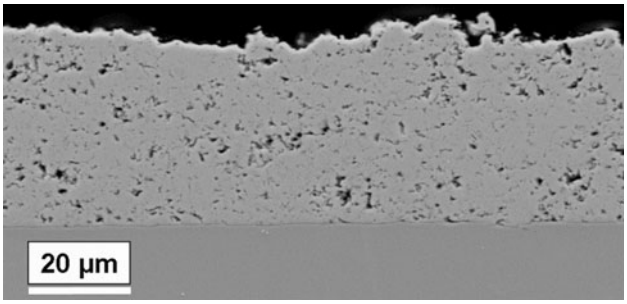

Fig. 7 Suspension plasma sprayed 8YSZ electrolyte layer with low porosity

open circuit voltage (OCV) for cells. At this, leak rate values were determined in a test rig at room temperature. One side of a sample with surface area A of the layer was exposed to atmospheric air pressure p_a. The other side was mounted to a chamber of constant volume V, which was evacuated to low pressure p_0 (≥300 Pa). While air from high pressure side moved into the chamber across the layer, pressures on both sides of the sample were detected. Starting from p_0 time interval Δt to equalize both pressures was measured. Finally area-related leak rate was given by

$$L_a = \frac{(p_a - p_0) \times V}{A \times \Delta t}$$

Despite this tremendous progress in plasma spraying of electrolytes further improvement is needed. For instance, the ionic conductivity of as-sprayed layers (0.021 S/cm) is threefold lower than plasma sprayed and sintered ones at 1500 °C for 4 h (0.068 S/cm). This was attributed to the splat boundaries which hinder ion diffusion across the deposit (Ref 15). In addition, post-mortem analysis of cells after long-term experiments showed increased formation of chromium oxide on the ferritic steel indicating that there was too much water on the cathode side of the cell (Ref 16). This corrosion is caused by extended cross-over of hydrogen and, hence, not sufficient gas-tightness of the electrolyte (see section 4). For this reason, first experiments of nanostructured electrolytes made by SPS were conducted to increase ion-conductivity as well as density. As can be seen in Fig. 7 it seems to be possible to get 8YSZ layers on dense substrates with low porosity. On adapting suspension plasma spray parameters (Table 1), a porosity of 6.7% could be measured by image analysis. However, Marr and Kesler (Ref 17) showed that electrolyte permeability behavior not only depends on spray parameters but also on surface quality of substrates used. Therefore, only electrochemical tests can finally give some more detailed information about the quality of these electrolyte coatings. These experiments are still pending.

3.2 Plasma Spraying of Cathodes

Although thickness and gas-tightness of the solid electrolyte are of high importance concerning ohmic resistance and degradation behavior of an SOFC the performance is also affected strongly by electrode layers.

Table 1 SPS conditions to get 8YSZ layers with low porosity on dense substrates

Current	400 A
Enthalpy	17.4 MJ/kg
Spray distance	90 mm
Suspension flow rate	38.4 mL/min

In case of limited porosity of plasma sprayed electrodes this causes lower gas permeability, obstructing mass transport within the electrodes and leading to high concentration polarization especially at higher current densities. In the end, it lowers power densities achievable. Therefore, experiments were done to increase porosity of cathodes in plasma sprayed cells.

As cathode material mainly $LaMnO_3$ or $LaCoO_3$ based perovskites are used [e.g., LSM ($La_{0.6}Sr_{0.4}MnO_3$) or LSCF ($La_{0.6}Sr_{0.4}Co_{0.2}Fe_{0.8}O_3$) (Ref 18)]. Again thermal spraying can be applied beneficially, as high temperatures (as used with sintering for instance) can be avoided which reduces the risk of undesirable interlayer reactions. In Ref 19 power densities at 0.7 V of more than 300 and 500 mW/cm^2 were reported for cells with LSM and LSCF cathodes produced by conventional plasma spraying with F4 type gun. In present work mixed nano-micro structured cathodes were developed. The nanometer-sized particles offered a high effective surface area for catalytic activity of gases. Nanoparticles, however, tend to agglomerate and sinter at operating temperatures of the cell and their beneficial effect can be quickly lost. Micrometer sized particle were, therefore, introduced to impede sintering of the nanoparticles. A 20 to 80 wt.% ratio of nanometer to micrometer-sized particles was adapted in which the nanometer-sized particles were 60 to 90 nm and micrometer-sized particles were 0.8 to 2 µm. The particles were agglomerated in size of 5 − 45 µm using spray drying prior to plasma spraying. Investigations with LSM ($La_{0.6}Sr_{0.4}MnO_3$) and LSCF ($La_{0.6}Sr_{0.4}Co_{0.2}Fe_{0.8}O_3$) as cathode material were carried out. These cathode deposits exhibited no undesirable secondary phases and sufficient permeability for gases (Ref 14).

However, perovskites may decompose at high temperatures and in reducing atmosphere forming secondary phases which are detrimental for electro-catalytic activity. Therefore, special care is needed during plasma spraying of these materials to avoid decomposition. Plasma enthalpy and plasma to particle heat transfer has to be limited. Otherwise severe degradation may reveal as can be seen in Fig. 8, where XRD measurements of $La_{0.58}Sr_{0.40}Co_{0.20}Fe_{0.80}O_3$ powder and different plasma sprayed deposits are shown (Table 2). Here plasma jet of parameter set 1 possessed a higher enthalpy, temperature and velocity compared to parameter set 2.

Reduction of enthalpy and velocity, however, may lead to extremely poor deposition efficiencies and rates. Therefore, another approach was considered that consisted of working with powder agglomerates instead of bulky particles. The spray process development was aiming at promoting partial melting of the surface of agglomerates while keeping the inner core unmelted. The

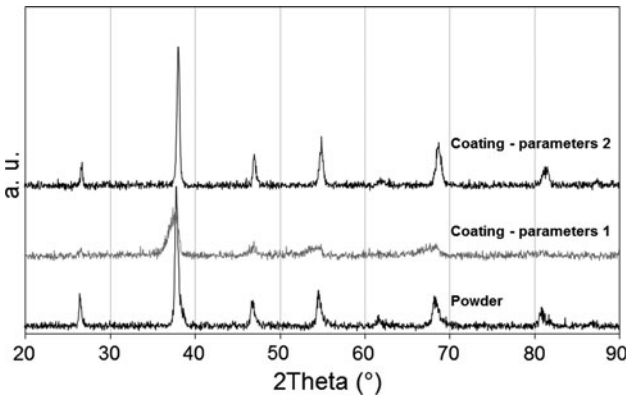

Fig. 8 XRD of $La_{0.58}Sr_{0.40}Co_{0.20}Fe_{0.80}O_3$ powder and resulting plasma sprayed deposits

Table 2 Plasma spray conditions for the fabrication of LSCF cathodes

	Anode diameter of plasma torch, mm	Ar flow rate, slm	He flow rate, slm	Arc current, A
1	11	30	5	350
2	9	50	5	200

molten surface acted in this way as an adhesive which assisted in sticking the impacting particles together. The porous interior provided the high specific surface area and the porosity for the deposit to ensure sufficient gas permeability and electrochemically active area. A porosity of around 20% with average pore radius of 0.84 μm and pore size range between 60 nm and 8 μm was achieved from identifying an appropriate set of processing parameters by correlating spray parameters to plasma jet characteristics, in-flight particle properties as well as deposit structure and quality. Furthermore, electrochemical testing with different types of LSCF materials ($La_{0.60}Sr_{0.40}Co_{0.20}Fe_{0.80}O_3$, $La_{0.58}Sr_{0.40}Co_{0.20}Fe_{0.80}O_3$ and $La_{0.78}Sr_{0.20}Co_{0.20}Fe_{0.80}O_3$) showed that powder stoichiometry and plasma spray parameters can strongly influence the electrochemical activity of the cathode layer especially at lower operating temperatures (Ref 10).

3.3 Suspension Plasma Spraying of Anodes

The anode is probably the most delicate functional layer of an SOFC with regard to the requirements it has to fulfill (Ref 20-22). On the one hand its electronic conductivity has to be as high as possible to minimize electric losses and supply electrons. If YSZ is used as electrolyte material the anode is normally a cermet consisting of nickel and YSZ. On the other hand, analogous to the cathode, it has to be porous enough to permit access of the fuel (mostly hydrogen or reformates from hydrocarbon fuels). The electrochemical performance of an anode layer is mainly governed by active reaction sites (TPB) where oxide ions from the electrolyte, fuel gas and electrode meet. These three phases do not only have to congregate in one point but for good electrochemical activity they

Table 3 8YSZ powders used for suspension plasma spraying of anodes

Powder distributor	Evonik (Darmstadt, Germany)	SAAN Innovations (Lund, Sweden)
Particle size	12 nm (“CITY”)	50 nm 200 nm
Dispersion medium	water	Ethanol/pentanol
Concentration	20 wt.%	10-20 wt.%

have to be connected to the electrolyte and the electronic contact layer by conducting paths of 8YSZ and nickel. Both conductivities depend on the content of nickel and, respectively, 8YSZ and are diametrically depending on their volume ratio (Ref 11). An optimal ratio (in vol.%) between 8YSZ and nickel is considered to be around 70/30 (Ref 23).

Another challenge for plasma sprayed MS-SOFC anodes is to possess a surface roughness as low as possible. The smoother the anode the thinner a gas-tight plasma sprayed electrolyte can be produced on top of it. Generally speaking the roughness in plasma spraying is limited by the splat characteristics and, thus, by the powder particle size. SPS shifts the lower particle size limit down to the nanometer scale and promises coatings with lower roughness. All reasons mentioned before (large active surface areas, good porosity, low roughness) were arguments to investigate SPS and SPPS as manufacturing process of anode layers.

Three 8YSZ powders were tested (Table 3). Under APS conditions nickel usually is sprayed as nickel oxide and is reduced to nickel before operating the fuel cell. However, nickel oxide melts at lower temperature than 8YSZ and is difficult to stabilize in a combined suspension with 8YSZ. Thus, nickel was applied by SPPS as nickel nitrate (hexahydrate) in liquid precursor form. This nitrate undergoes different stages from liquid precipitation and oxidation until melting of the resulting nickel oxide (Ref 24-26). To control the formation of a composite cermet structure of nickel oxide and 8YSZ the behavior of each liquid had to be investigated separately. In the following the injection of nickel nitrate will be discussed first.

Depending on spray distance liquid nickel nitrate injected shows an increase of weight of nickel oxide on steel substrates (Fig. 9). The sharp peak at 80 mm spray distance is the point of optimum particle conditioning. Most of the liquid precursor has transformed into fully molten nickel oxide droplets and, thus, an optimal deposition rate is reached. The lower deposition at smaller distances can be attributed to unfinished precipitation or melting of light small particles, whereas the strong decline after 80 mm is an indication for cooling and decelerating particles. Similar effects are already known from plasma spraying with >10 μm powders at spray distances from 100 to 120 mm as discussed in Ref 27. The only difference is that melting and cooling happens there within centimeters not millimeters. The same behavior is reflected in the roughness of the coating. At a spray distance of 55 mm the roughness is lower because only smaller precursor droplets have

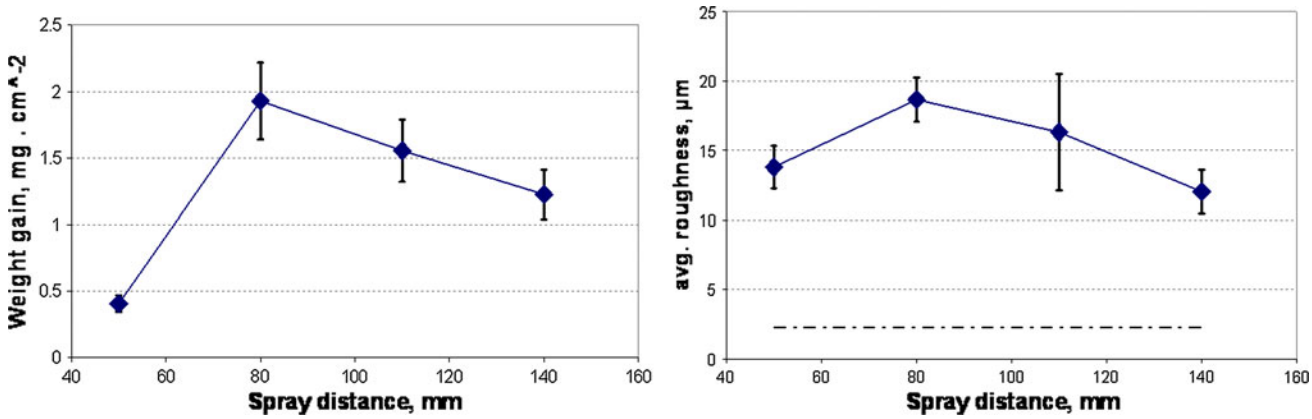

Fig. 9 Exemplary deposition and roughness characteristics of nickel nitrate over increasing spraying distance (200 A, 50 slm Ar, 46 mL/min of 10 wt.% Ni)

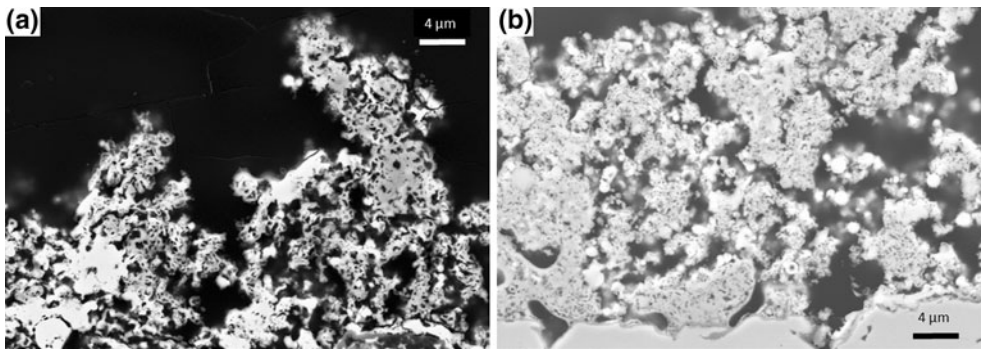

Fig. 10 Nickel nitrate layer deposited by SPPS of (a) hollow and (b) compact broken spheres

transformed into molten particles or liquid precursors have precipitated on the substrate.

However, the roughness is higher than expected for coatings made of nanoparticles because the droplets did not transform into solid particles but into hollow spheres with diameters in the range of droplets of 10 µm. After 80 mm those shells solidify, break and form denser and smoother layers. Figure 10 shows cross sections of both stages in SEM. In Fig. 10(a) cavities of micrometer size can be seen that are formed when hollow shells of nickel oxide collide with the substrate. Once the spheres cool down after 80 mm their elasticity is reduced and denser structures arise as seen in Fig. 10(b).

In contrast to nickel nitrate SPS coatings made by injection of 8YSZ nanoparticles in a water-based suspension show a completely different behavior. Referring to 28 and 29 no local maximum of deposition can be found for different spray distances when they are too large for nanoparticles, or if thermal loading on substrate is too high at closer distances. In Fig. 11 the declining branch of the deposition behavior similar to the one of Fig. 9 after 80 mm can be seen. In contrast to nickel nitrate injection the roughness is in general very low for all distances. This is a direct result of the particle size of the powder used in the suspension. They can form finer splats than powders in conventional plasma spraying and can even compensate substrate roughness. What is needed to get a coating with a smooth surface is, therefore, a nanopowder that stays in agglomerated form with a semi molten shell. If the agglomerate hits the surface, its outer molten shell breaks, releases the not fully melted nanoparticles and sticks them onto the substrate. In this respect, the process differs strongly from a coating process with fully molten agglomerates which lead to micrometer or sub-micrometer particles. Sub-micrometer particles, however, tend to mimic the substrate roughness up to several microns coating thickness. This effect has become familiar under the name ''stacking defects'' in SPS coatings (Ref 30, 31).

In the next step both liquids were injected simultaneously for plasma sprayed fuel cell anodes. The coatings were optimized for a Ni/Zr volume ratio of 1:2 which was investigated by XRD. Furthermore, the resulting coating roughness was measured. Out of 200 parameter sets tested in a first trial three of them were chosen according to different roughness and thickness which are the result of a differing microstructure. Spray parameters and coating compositions are listed in Table 4. The coatings were not optimized for getting a high porosity. This will be created later on during the reduction of nickel oxide which leads to a volume shrinkage of nickel oxide to nickel by 40%.

All anodes were coated at the same time with a VPS electrolyte layer showing similar leak rates of about

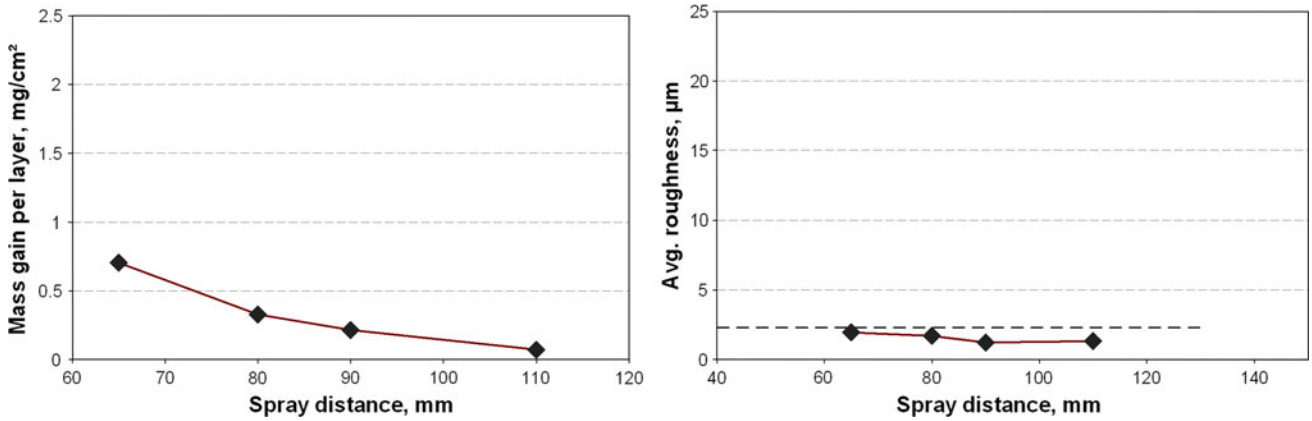

Fig. 11 Exemplary deposition and roughness characteristics of 8YSZ (SAAN) with increasing spraying distance (500 A, 50 slm Ar, 30 mL/min of 10 wt.% 8YSZ)

Table 4 SPS parameters tested for anode layer

Sample no.	A	B	C
Torch current, A	500	400	400
Ar flow rate, slm	70	70	50
He flow rate, slm	…	…	20
Flow rate (nickel nitrate), mL/min	46.2	23.0	28.0
Distance torch to sample, mm	75	65	65
Amount of NiO in anode, wt.%	38.83	40.64	43.52
Amount of YSZ in anode, wt.%	61.17	59.36	56.48
Roughness R_a of anode surface, µm	5.8	5.9	3.4
Avg. thickness of anode, µm	12	10	9

4.5 Pa m/s. LSCF paste was brushed manually as cathode layer and contacting was done with a platinum mesh. The cells had a diameter of 40 mm. Roughness R_a of anode surface and average thickness of anode is given in Table 4. Cross-sections of the complete fuel cell after testing are shown in Fig. 12. Anode A mainly consists of fully molten splats of nickel oxide and 8YSZ. This explains the mimicking effect of the substrate and the highest roughness among all tested anodes. Anode B and C consist mostly of fully molten nickel oxide and partially molten 8YSZ agglomerates, which fill the gaps of the substrate and lead to a smoother anode surface.

First results of these newly developed anode layers are shown as *U-i* curves in Fig. 13. Maximum power density at 0.7 V could be detected in cell B (66.9 mW/cm^2). The value of cell C is similar under same conditions (65.4 mW/cm^2), whereas cell A performs poorest with only 49.3 mW/cm^2. Even though the performance is only one-tenth of what conventionally sprayed cells perform, a clear distinction can be found between microstructural factors influencing the performance. Cell B and C perform very similar though their anode microstructure is very different. Anode of cell B is rougher and slightly thicker than anode of cell C. Since performance is similar, it seems that some properties changed diametrically. However, to get a more conclusive picture further examinations by electrochemical impedance spectroscopy are planned to reveal more details about the chemical reaction mechanisms and their limiting properties.

4. Improvements Achieved in Metal-Supported SOFCs

The main requirements on MS-SOFC, and according to the functional layers it consists of, are high electrical power densities, good mechanical stability and durability for long-term operation, i.e., mainly stable against thermal and redox-cycling. All spray activities described in section 3 served to implement these requirements. In combining such plasma sprayed electrolytes with improved plasma sprayed electrodes, at operation temperatures of 800 °C power densities of around 800 mW/cm^2 at 0.7 V for small single cells (12.56 cm^2), around 400 mW/cm^2 at 0.7 V for 80 cm^2 cells and >300 mW/cm^2 at 0.7 V in a 250 W stack made of 10 cells could be successfully demonstrated. As an example the development of maximum power density of plasma sprayed single cells at DLR between 2006 and 2010 is shown in Fig. 14. Further improvements in power density are expected in future by previously shown potential in liquid injection plasma spraying of functional layers. However, prior to this, activities at DLR have been concentrated on testing the durability of plasma sprayed MS-SOFC stacks for long-term operation.

Plasma sprayed MS-SOFC stacks show a superior resistance to strong temperature and redox-cycling tests compared to conventionally made ones. A strong anode reduction, e.g., was done in switching off the fuel gas abruptly and purging immediately with nitrogen for 5 min to remove residual hydrogen. Subsequently, anode side was flowed through with 50 mL/min pure oxygen for 1 h to oxidize the nickel inside. Before running the stack again with standard fuel gas (1 slm H_2 and 1 slm N_2) it was purged with nitrogen once more. 20 of such redox-cycles together with 15 thermal cycles could be reached in one MS-SOFC stack made of 10 cells (Fig. 15). Between individual cycles the degradation rate was determined from polarization curves at OCV. Subsequently, a load of 200 mA/cm^2 was applied for one hour. The increase of power after two redox-cycles can probably be explained by a breakup of the nickel agglomerates inside the anode

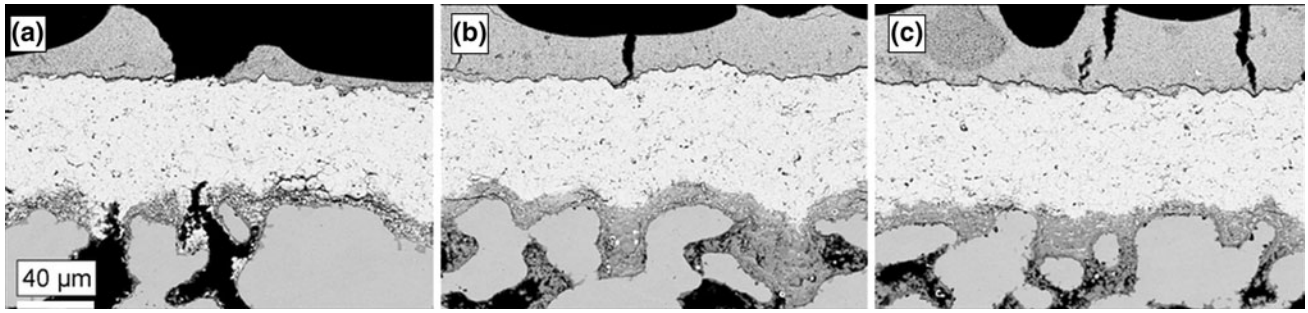

Fig. 12 SEM pictures of cross-section polish of tested fuel cells: A = high, B = medium, C = low roughness of anode

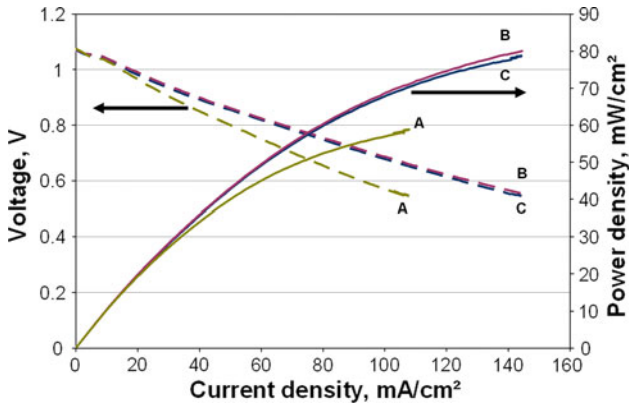

Fig. 13 So-called ''*U-i*-curves'' (a combined diagram of polarization (dashed) and power density curves (solid)) of tested fuel cells with varying anode layers (800 °C, 2 slm H_2 with 2 slm N_2 on anode side, 8 slm O_2 on cathode side)

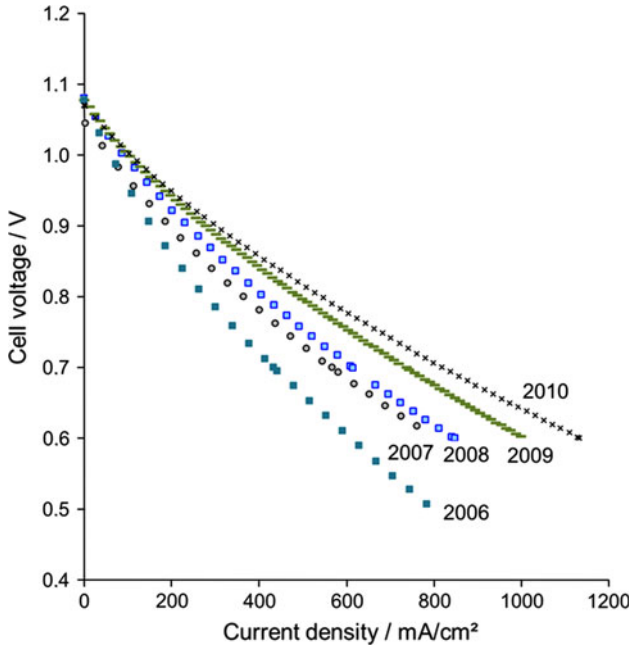

Fig. 14 Development of maximum power density of plasma sprayed single cells at DLR between 2006 and 2010

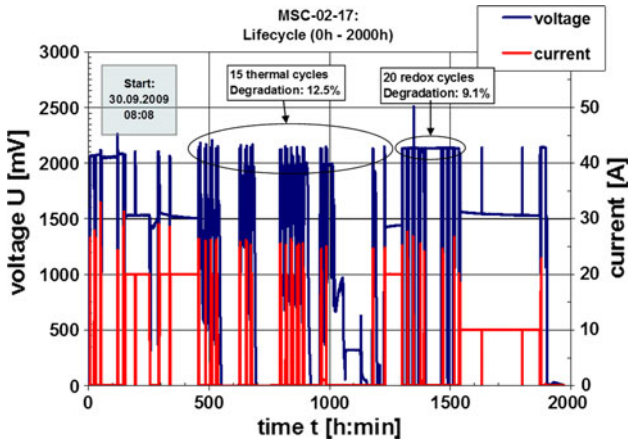

Fig. 15 MS-SOFC stack made of 10 cells tested under conditions of thermal and redox-cycling

increasing TPB. However, with increasing number of cycles this effect was compensated by a degradation of the anode. This degradation manifested in appearance of micro cracks caused by volume changes during redox-cycling. The degradation rate after 20 cycles was 9.1%.

One limiting factor of plasma sprayed MS-SOFCs remains: gas-tightness of the electrolyte layer restricts the diminishing of layer thickness. Insufficient gas-tightness to hydrogen diffusion does not only reduce the efficiency of the cell but may also limit life-time of the cell, as water is produced at the cathode side. This water can corrode the interconnector made of ODS-Fe26Cr alloy (ITM) and can lead to chromium poisoning of the cell. Interestingly, an endurance test at DLR on a plasma sprayed MS-SOFC stack with four cells showed that an operating time of more than 5000 h was possible (Fig. 16). Although the overall degradation rate was 10.7% (~4%/1000 h during the first 2500 h), which is still too high for industrial applications, this was a promising value as no protective coatings were used in this stack. Future investigations on an MS-SOFC stack with protective coatings on cathode side and diffusion barrier layer on anode side are expected to provide much lower degradation rates and, thus, longer operating times.

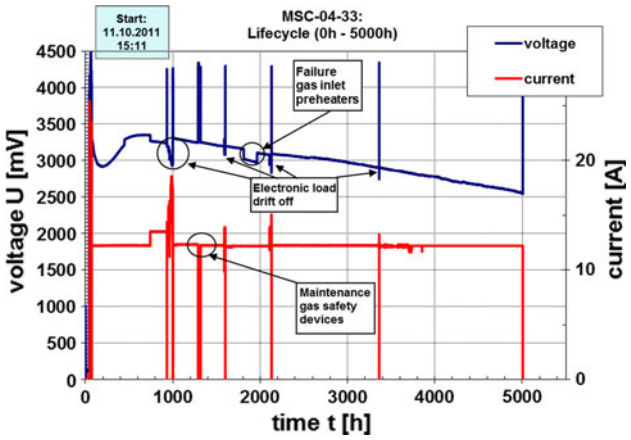

Fig. 16 Endurance test on MS-SOFC stack with four cells

5. Conclusion

Results presented in this paper support that plasma spraying can be a promising alternative to wet ceramic processing. However, each functional layer needs a customized approach of plasma spraying. Only conventional APS technology with micrometer-sized powders is not sufficient to get highest qualities of coatings. It was shown in this work that VPS, SPS as well as SPPS and combinations thereof are promising alternatives especially for gas-tight thin electrolyte and high-efficient electrode layers. It could be demonstrated that plasma sprayed MS-SOFCs can be prepared having power densities approaching those of main stream anode supported cells often produced by wet ceramic processes. Despite of continuous enhancements of power density and long-term stability over the last years that were presented in this paper, durability of plasma sprayed MS-SOFC (e.g. degradation) still has to be further improved to make plasma spraying a predominant manufacturing technique. At the same time, the costs and complexity of handling these spray technologies have to be considered to become successfully implemented in industrial mass production.

Acknowledgments

The results presented here were obtained within the framework of several projects funded by the German Ministry of Economic Affairs and Technology. The authors gratefully acknowledge Volker Thielke, Günter Roth, Gudrun Steinhilber and Ina Plock from DLR Stuttgart for their valuable contributions to this work.

References

1. H. Gruner and H. Tannenberger, Plasma gespritzte Schichten für Brennstoffzellentechniken [Plasma Sprayed Coatings for Fuel Cell Techniques], *DVS-Bericht*, 1990, **130**, p 194-196 [in German]
2. W. Mallener, K. Wippermann, H. Jansen, Z. Li, and D. Stöver, VPS Fabrication of Electroactive Solid Oxide Fuel Cell Membranes, *Thermal Spray: International Advances in Coatings Technology*, C. C. Berndt, ASM International (Orlando, FL), 1992, May 25-June 5, 1992, p 835-838
3. R. Henne, E. Fendler, and M. Lang, Potential of Vacuum Plasma Spraying for the Production of SOFC Components, *Proceedings of the 1st European Solid Oxide Fuel Cell Conference*, Lucerne (Switzerland), 1994, p 612-627
4. T. Franco, Entwicklung und Charakterisierung von anodenseitigen Diffusionsbarriereschichten für metallgetragene oxidkeramische Festelektrolyt-Brennstoffzellen [Development and characterization of Diffusion Barrier Layers for Metal-Supported Solid Oxide Fuel Cells], Stuttgart: epubli, 2009 [in German]
5. J. Arnold, S. A. Ansar, U. Maier, and R. Henne, Insulating and Sealing of SOFC Devices by Plasma Sprayed Ceramic Layers, *International Thermal Spray Conference & Exposition, Thermal Spray 2008: Crossing Borders (DVS-ASM)* (Maastricht, The Netherlands), 02-04 June 2008, p 83-87
6. R. Henne, Solid Oxide Fuel Cells: A Challenge for Plasma Deposition Processes, *J. Therm. Spray Technol.*, 2007, **16**(3), p 381-403
7. J. Arnold and S.A. Ansar, Plasma-Sprayed Coatings in Solid Oxide Fuel Cells, *Thermal Spray Bulletin*, 2/2012, p 110-116
8. R. Vaßen, D. Hathiramani, J. Mertens, V. Haanappel, and I. Vinke, Manufacturing of High Performance SOFCs with Atmospheric Plasma Spraying (APS), *Surf. Coat. Technol.*, 2007, **202**, p 499-508
9. J. Arnold, S.A. Ansar, R. Ruckdäschel, R. Henne, U. Maier, and H.W. Grünling, Vacuum Plasma Sprayed Insulating Layers Suitable for Brazing in High Temperature Fuel Cells, *Abstracts and Manuscripts of the ITSC-Conference 2011 in Hamburg*, No. 276, 27-29 September 2011, p 143-148
10. A. Ansar, D. Soysal, Z. Ilhan, and N. Wagner, Plasma Sprayed LSCF Oxygen Electrode for SOFC, *International Thermal Spray Conference & Exposition, Thermal Spray 2010: Global Solutions for Future Application (DVS-ASM)* (Singapore), 03-05 May 2010, p 108-113
11. H. Weckmann, A.A. Syed, Z. Ilhan, and J. Arnold, Development of Porous Anode Layers for the Solid Oxide Fuel Cell by Plasma Spraying, *J. Therm. Spray Technol.*, 2006, **15**(4), p 604-609
12. L. Jia, C. Dossou-Yovo, C. Gahlehrt, and F. Gitzhofer, Induction Plasma Spraying of Samarium Doped Ceria as Electrolyte for Solid Oxide Fuel Cells, *Thermal Spray 2004: Advances in Technology and Application*, ASM International (Osaka, Japan), May 10-12, 2004, p 85-89
13. D. Stolten, *Hydrogen and Fuel Cells*, Wiley-VCH Verlag GmbH & Co KGaA, Weinheim (Germany), 2010
14. S. A. Ansar, Z. Ilhan, and J. Arnold, Plasma Sprayed Metal Supported SOFCs Having Enhanced Performance and Durability, *International Thermal Spray Conference*, Las Vegas, USA, 2009
15. C. Christenn and S.A. Ansar, Sprayed and Constrained-Sintered Zirconia Based Electrolytes, *Thermal Spray 2009: Expanding Thermal Spray Performance to New Markets and Applications*, ASM International, May 2009, p 131-135
16. M. Garcia-Vargas, L. Lelait, V. Kolarik, H. Fietzek, and Md Mar Juez-Lorenzo, Oxidation of Potential SOFC Interconnect Materials, Crofer 22 APU and Avesta 353 MA, in Dry and Humid Air Studied In Situ by X-ray Diffraction, *Mater. High Temp.*, 2005, **22**(3/4), p 245-251
17. M. Marr and O. Kesler, Permeability and Microstructure of Suspension Plasma-Sprayed YSZ Electrolytes for SOFCs on Various Substrates, *J. Therm. Spray Technol.*, 2012, **21**(6), p 1334-1346
18. Y. Shen, V.A.B. Almeida, and F. Gitzhofer, Preparation of Nanocomposite GDC/LSCF Cathode Material for IT-SOFC by Induction Plasma Spraying, *J. Therm. Spray Technol.*, 2011, **20**(1-2), p 145-153
19. S.A. Ansar, Z. Ilhan, G. Schiller, O. Patz, and J.B. Gregoire, Plasma Sprayed Oxygen Electrode for Solid Oxide Fuel Cells and High Temperature Water Electrolyzers, *International Thermal Spray Conference & Exposition*, Maastricht, The Netherlands, 2008
20. T. Suzuki, Z. Hasan, Y. Funahashi, T. Yamaguchi, Y. Fujishiro, and M. Awano, Impact of Anode Microstructure on Solid Oxide Fuel Cells, *Science*, 2009, **325**(5942), p 852-855
21. A. Faes, A. Hessler-Wyser, D. Presvytes, C.G. Vayenas, and J.V. herle, Nickel-Zirconia Anode Degradation and Triple Phase

Boundary Quantification from Microstructural Analysis, *Fuel Cells*, 2009, **09**(6), p 841-851
22. N. Oishi and Y. Yoo, Evaluation of Metal Supported Ceria Based Solid Oxide Fuel Cell Fabricated by Wet Powder Spray and Sintering, *J. Electrochem. Soc.*, 2010, **157**(1), p B125-B129
23. H. Koide, Y. Someya, T. Yoshida, and T. Maruyama, Properties of Ni/YSZ Cermet as Anode for SOFC, *Solid State Ionics*, 2000, **132**(3-4), p 253-260
24. A. Vardelle, C. Chazelas, C. Marchand, and G. Mariaux, Modeling Time-Dependent Phenomena in Plasma Spraying of Liquid Precursors, *Pure Appl. Chem.*, 2008, **80**(9), p 1981-1991
25. A. Saha, S. Seal, B. Cetegen, E. Jordan, A. Ozturk, and S. Basu, Thermo-Physical Processes in Cerium Nitrate Precursor Droplets Injected into High Temperature Plasma, *Surf. Coat. Technol.*, 2009, **203**(15), p 2081-2091
26. C. Marchand, A. Vardelle, G. Mariaux, and P. Lefort, Modelling of the Plasma Spray Process with Liquid Feedstock Injection, *Surf. Coat. Technol.*, 2008, **202**(18), p 4458-4464
27. P. Fauchais, V. Rat, J.-F. Coudert, R. Etchart-Salas, and G. Montavon, Operating Parameters for Suspension and Solution Plasma-Spray Coatings, *Surf. Coat. Technol.*, 2008, **202**(18), p 4309-4317
28. L. Pawlowski, Suspension and Solution Thermal Spray Coatings, *Surf. Coat. Technol.*, 2009, **203**(19), p 2807-2829
29. R. Vaßen, H. Kaßner, G. Mauer, and D. Stöver, Suspension Plasma Spraying: Process Characteristics and Applications, *J. Therm. Spray Technol.*, 2009, **19**(1-2), p 219-225
30. P. Fauchais, R. Etchart-Salas, V. Rat, J.F. Coudert, N. Caron, and K. Wittmann-Ténèze, Parameters Controlling Liquid Plasma Spraying: Solutions, Sols, or Suspensions, *J. Therm. Spray Technol.*, 2008, **17**(1), p 31-59
31. A. Bacciochini, G. Montavon, J. Ilavsky, A. Denoirjean, and P. Fauchais, Porous Architecture of SPS Thick YSZ Coatings Structured at the Nanometer Scale (~50 nm), *J. Therm. Spray Technol.*, 2009, **19**(1-2), p 198-206